ACADEMIC PRESS

Available online at www.sciencedirect.com

SCIENCE DIRECT®

Journal of Sound and Vibration 261 (2003) 17–29

JOURNAL OF SOUND AND VIBRATION

www.elsevier.com/locate/jsvi

Crack detection in hollow section structures through coupled response measurements

D. Liu[a,b,*], H. Gurgenci[a,b], M. Veidt[b]

[a] *Cooperative Research Centre for Mining Technology and Equipment, Kenmore, QLD 4069, Australia*
[b] *Department of Mechanical Engineering, The University of Queensland, Staff House Road, Building 45, Room 204, St. Lucia, QLD 4072, Australia*

Received 31 August 2001; accepted 15 May 2002

Abstract

Detection of a circumferential crack in a hollow section beam is investigated using coupled response measurements. The crack section is represented by a local flexibility matrix connecting two undamaged beam segments. This matrix defines the relationship between the displacements and forces across the crack section and is derived by applying fundamental fracture mechanics theory. The suitability of the mode coupling methodology is first demonstrated analytically. Laboratory test results are then presented for circular hollow section beams with artificially generated cracks of varying severity. It is shown that this method has the potential as a damage detection tool for mechanical structures.

1. Introduction

Detection and control of damage in mechanical structures is an important concern to engineering communities. Among many possible damage identification methods, vibration measurements offer the potential to be an effective, inexpensive and fast tool for non-destructive testing. During the past several decades, significant amount of research has been conducted in the area of vibration-based damage identification. The main idea of this approach is that a change in a system due to damage will manifest itself as changes in the structural dynamic characteristics.

Reviews on vibration of cracked structures were reported by Dimarogonas [1], Wauer [2] and Doebling et al. [3]. Many identification techniques have been proposed based on different system

*Corresponding author. Department of Mechanical Engineering, The University of Queensland, Staff House Road, Building 45, Room 204, St. Lucia, QLD 4072, Australia.
E-mail address: liu@mech.uq.edu.au (D. Liu).

0022-460X/03/$ - see front matter
PII: S0022-460X(02)00922-7

parameters. Some authors used the change of natural frequencies [4–6] or mode shapes [7,8] as the indicator of damage while others detected structural damage directly from dynamic response in time domain or from frequency response functions (FRF) [9]. Despite a certain degree of success with these techniques, a common observation derived from the above studies is the relative insensitivity of global parameters such as mode shapes and frequencies to local damage.

In this paper, we examine the suitability of using coupled responses to detect damage in thin-walled tubular structures. By coupled response we refer to the ability of a structural member with a circumferential crack to experience composite vibration modes (axial and bending) when excited purely laterally. These composite modes are only present when there is a crack.

The starting point in this approach is modelling the crack section. We use a local flexibility matrix. This matrix defines the relationship between the displacements and forces as shown in Eq. (1). It can be formulated as a function of the stress intensity factors using fundamental fracture mechanics theory [10–13].

Generally, for uncracked members the local flexibility matrix is diagonal. In the presence of a crack, some off-diagonal terms become non-zero. This means excitation along one direction (e.g., lateral) will cause response along other directions (e.g., axial).

The simple case of local flexibility was studied by Irwin [14] for beams and by Rice and Levy [15] for plates, who related the flexibility to stress intensity factors. Papadopoulos and Dimarogonas [16] presented the comprehensive solution of coupled vibration in a cracked shaft. But the available results were mostly based on analytical simulations with no experimental verification and only solid section structures were considered. In fact, all past work in this area has been limited to solid beams, e.g., turbine or impeller blades.

In welded mechanical and civil structures, hollow or open sections are usually the preferred shape rather than solid beams. In this paper, a coupled-response of a Circular Hollow Section (CHS) beam due to circumferential cracks is studied both analytically and experimentally. After first deriving the local flexibility matrix, analytical simulations of free and forced vibrations of cracked CHS beams are presented and the efficacy of the proposed coupling property in crack identification is demonstrated. The results for different crack severities and locations are compared based on analytical simulations. Finally, the results of laboratory tests on a similar geometry are presented to show the feasibility of this approach. Standard modal validation techniques are used to interpret the coupled modes caused by the crack.

2. Local flexibility matrix and axial–bending coupling coefficients of a CHS member

A crack in a structural member introduces additional local flexibility, which is a function of the crack depth (severity) and location. In this study, the focus is on circumferential cracks encountered in CHS beams. The severity of the crack is represented by the ratio of the crack area to the total cross-sectional area. For example, a 10% crack represents the loss of 10% of the cross-sectional area of the beam. The extra flexibility introduced by the crack changes the dynamic behaviour of the system. To see how this happens, one has

to first establish the local stiffness or flexibility matrix of the cracked member under general loading.

In general, the local flexibility of a beam at any single point can be described by inserting a virtual joint at that point and representing that joint by a local flexibility matrix. The matrix size depends on the number of the degrees of freedom being considered for the joint, the maximum being 6×6. The co-ordinate system and the corresponding generalised forces are shown in Fig. 1. Here subscript 1 is used for the longitudinal force, 2 and 3 for the shearing forces, 4 and 5 for the bending moments and 6 for the torsional moment. Using the local flexibility matrix, the extra displacement along any degree of freedom due to the presence of the crack is given by the following equation:

$$\vec{u} = C\vec{P}, \tag{1}$$

where $\vec{u}$ and $\vec{P}$ are displacement and force vectors and C is the local flexibility matrix: $\vec{u} \in R^{6\times1}$; $C \in R^{6\times6}$; $\vec{P} \in R^{6\times1}$. The length of the beam and the location of the crack are shown as L and l, respectively, in Fig. 1.

The displacement u_i along the force component P_i due to the presence of the crack is computed using Castigliano's theorem as described in Ref. [11]. The general expression for the local flexibility coefficients is

$$c_{ij} = \frac{1}{E'}\int_0^a \left[\frac{\partial^2}{\partial P_i \partial P_j}\sum_{m=I}^{III} e_m \left(\sum_{n=1}^{6} K_{mn}\right)^2\right] \mathrm{d}x, \tag{2}$$

where $E' = E$ for plane stress, $E' = E/(1-v^2)$ for plane strain; $\alpha = 1+v$; E and v are Young's modulus and Poisson's ratio, respectively; $e_m = 1$ for $m = \mathrm{I}, \mathrm{II}$ and $e_m = \alpha$ for $m = \mathrm{III}$; K_{mn} is the stress intensity factor of mode m ($m = \mathrm{I}, \mathrm{II}, \mathrm{III}$) due to the load P_n ($n = 1, 2, \ldots, 6$); a is the length along the crack tip.

From Eq. (2), the existence of coupling between two vibration modes is described by the magnitude of the corresponding K_{mn} coefficient. If some of the loads contribute to the same fracture mode, for example, beam under extension and bending both create tensile stress and contribute to mode I of stress intensity factor (i.e., $K_{\mathrm{I}1} \neq 0, K_{\mathrm{I}5} \neq 0$), the corresponding flexibility element would be non-zero (i.e., $c_{15} \neq 0$).

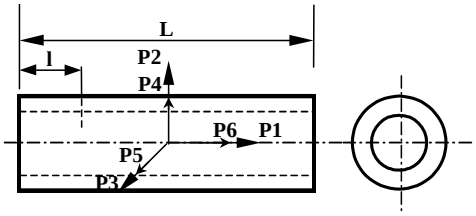

Fig. 1. CHS beam under general loading

Thus, the local flexibility matrix for the beam due to the crack has the following form:

$$C = \begin{bmatrix} c_{11} & 0 & 0 & c_{14} & c_{15} & 0 \\ 0 & c_{22} & 0 & 0 & 0 & c_{26} \\ 0 & 0 & c_{33} & 0 & 0 & c_{36} \\ c_{41} & 0 & 0 & c_{44} & c_{45} & 0 \\ c_{51} & 0 & 0 & c_{54} & c_{55} & 0 \\ 0 & c_{62} & c_{63} & 0 & 0 & c_{66} \end{bmatrix}. \tag{3}$$

This matrix relates the displacement vector $\{u\}$ to the corresponding force vector $\{P\}$ through Eq. (1).

By inversion of this local flexibility matrix we can obtain the local stiffness matrix:

$$K = C^{-1} \tag{4}$$

Due to reciprocity, the matrix C and K are symmetric for an uncracked beam. The non-diagonal terms of the matrix C show that coupling exists between longitudinal, bending and torsional vibrations because of the crack.

As shown in Eq. (2), the calculation of the local flexibility matrix is based on the relevant stress intensity factors. In this paper, coupling between longitudinal and bending vibration is considered, i.e., the analysis is restricted to two degrees of freedom, and the $2 \times 2 C$ and K matrices can be expressed as

$$C = \begin{bmatrix} c_{11} & c_{15} \\ c_{51} & c_{55} \end{bmatrix}, \quad K = \begin{bmatrix} k_{11} & k_{15} \\ k_{51} & k_{55} \end{bmatrix}. \tag{5}$$

Using fracture mechanics [10] principles, the stress intensity factors for a circumferential through-wall crack in cylinders can be expressed as follows:

Axial force P_1:

$$K_{\mathrm{I}1} = \frac{P_1}{2\pi R t}\sqrt{\pi R\theta}F_t, \tag{6}$$

where $R = (R_o + R_i)/2$ is the mean radius; and θ is the half-angle of the total through-wall crack (the crack severity will be indicated by θ/π as percentage) and

$$F_t = 1 + A_t\left[5.3303\left(\frac{\theta}{\pi}\right)^{1.5} + 18.773\left(\frac{\theta}{\pi}\right)^{4.24}\right],$$

where

$$A_t = \left(0.125\frac{R}{t} - 0.25\right)^{0.25} \quad \text{for } 5 \leqslant \frac{R}{t} \leqslant 10,$$

$$A_t = \left(0.4\frac{R}{t} - 3.0\right)^{0.25} \quad \text{for } 10 \leqslant \frac{R}{t} \leqslant 20.$$

Bending moment P_5

$$K_{I5} = \frac{P_5}{\pi R^2 t}\sqrt{\pi R\theta}F_b, \tag{7}$$

where

$$F_b = 1 + A_t\left[4.5967\left(\frac{\theta}{\pi}\right)^{1.5} + 2.6422\left(\frac{\theta}{\pi}\right)^{4.24}\right],$$

A_t is same as above.

Substituting K_{I1} and K_{I5} to Eq. (2) yields the coefficients C_{ij} by analytical or numerical integration. The C and K matrices can be derived according to Eqs. (3) and (4). Once the local flexibility matrix is obtained, the vibration modes of a cracked CHS beam can be developed using classical beam theory.

3. Free vibration of a cracked CHS beam

In this paper, we will consider a free–free beam. This is done to facilitate ready comparison between analytical and experimental results without having to consider the effect of the boundary conditions. The experiments were conducted in free–free boundary conditions. If required, the treatment can easily be adjusted to model different boundary conditions.

The vibration of a free–free Euler–Bernoulli CHS beam are described by the following differential equations:

Axial vibration:

$$\frac{\partial^2 U_i}{\partial x^2} = \frac{\rho}{E}\frac{\partial^2 U_i}{\partial t^2}, \quad i = 1, 2. \tag{8}$$

Lateral vibration:

$$\frac{\partial^4 V_i}{\partial x^4} + \frac{\rho A}{EI}\frac{\partial^2 V_i}{\partial t^2} = 0, \quad i = 1, 2, \tag{9}$$

where U_i and V_i are the axial and lateral displacements, respectively; $i = 1$ represents the section left to the crack ($x \leqslant l$) and $i = 2$ represents the section right to the crack ($l \leqslant x \leqslant L$).

The derivation follows closely traditional Euler–Bernoulli beam theory including continuity conditions at the crack section. Applying general variable separation technique, the solutions to Eqs. (8) and (9) are

$$U_1(x, t) = u_1(x)(A_u \cos \omega t + B_u \sin \omega t), \tag{10}$$

$$U_2(x, t) = u_2(x)(A_u \cos \omega t + B_u \sin \omega t), \tag{11}$$

$$V_1(x, t) = v_1(x)(A_v \cos \omega t + B_v \sin \omega t), \tag{12}$$

$$V_2(x, t) = v_2(x)(A_v \cos \omega t + B_v \sin \omega t), \tag{13}$$

where ω is the natural frequency of the system, A_u, B_u, A_v, $B_v$are unknown coefficients to be determined from the initial conditions, and u_i, v_i $(i = 1, 2)$ are unknown mode shapes.

Substituting Eqs. (10)–(13) into Eqs. (8) and (9) the governing equations for u_i, v_i are obtained as

$$\frac{\partial^2 u_1}{\partial x^2} + k_u^2 u_1 = 0, \tag{14}$$

$$\frac{\partial^2 u_2}{\partial x^2} + k_u^2 u_2 = 0, \tag{15}$$

$$\frac{\partial^4 v_1}{\partial x^4} - k_v^4 v_1 = 0, \tag{16}$$

$$\frac{\partial^4 v_2}{\partial x^4} - k_v^4 v_2 = 0, \tag{17}$$

where

$$k_u = \sqrt{\frac{\rho}{E}}\omega, \quad k_v = \left(\frac{\rho A \omega^2}{EI}\right)^{1/4}.$$

The general solutions of Eqs. (14)–(17) have the following form:

$$u_1(x) = A_1 \cos k_u x + A_2 \sin k_u x, \tag{18}$$

$$u_2(x) = A_3 \cos k_u x + A_4 \sin k_u x, \tag{19}$$

$$v_1(x) = A_5 \cosh k_v x + A_6 \sinh k_v x + A_7 \cos k_v x + A_8 \sin k_v x, \tag{20}$$

$$v_2(x) = A_9 \cosh k_v x + A_{10} \sinh k_v x + A_{11} \cos k_v x + A_{12} \sin k_v x, \tag{21}$$

where $A_i, i = 1, 2, \ldots, 12$ are unknown coefficients that are determined using the boundary and crack discontinuity conditions. Considering a beam with a small crack, the boundaries include both ends and the two sides of the crack (totally 12 conditions).

For a cracked free–free beam, the boundary conditions are given by Eqs. (22)–(29). At the free ends, the axial force, bending moment and shearing force are zero:

Free end 1 ($x = 0$):

$$AEu_1'(0) = 0, \tag{22a}$$

$$EIv_1''(0) = 0, \tag{22b}$$

$$EIv_1'''(0) = 0. \tag{22c}$$

Free end 2 ($x = L$):

$$AEu_2'(L) = 0, \quad EIv_2''(L) = 0, \quad EIv_2'''(L) = 0. \tag{23a–c}$$

At the crack section, there is continuity of axial force (Eq. (24)), bending moment (25), shearing force (26) and lateral displacement (27).

$$AEu_1'(l) = AEu_2'(l), \tag{24}$$

$$EIv_1''(l) = EIv_2''(l), \tag{25}$$

$$EIv_1'''(l) = EIv_2'''(l), \tag{26}$$

$$v_1(l) = v_2(l). \tag{27}$$

However, the axial displacement and the lateral slope are discontinuous. The relationship with respect to axial force and bending moment are shown as Eqs. (28) and (29), respectively.

$$AEu_1'(l) = k_{11}[u_2(l) - u_1(l)] + k_{15}[v_2'(l) - v_1'(l)], \tag{28}$$

$$EIv_1''(l) = k_{51}[u_2(l) - u_1(l)] + k_{55}[v_2'(l) - v_1'(l)]. \tag{29}$$

Eqs. (28) and (29) demonstrate the coupling between axial and lateral vibrations. The coefficients k_{ij} are the elements in the local stiffness matrix K (Eq. (5)), which is related to the local flexibility matrix C through Eq. (4).

Substitution of solutions (18)–(21) into the boundary conditions (22)–(29) yields 12 homogeneous algebraic equations for $A_1, A_2, \ldots, A_{12}$. Existence of non-trivial solutions requires the determinant of the coefficient matrix to be zero, which yields an equation for the determination of the system's natural frequencies ω_i. For each value of ω_i the corresponding axial and bending mode shapes are determined using Eqs. (18)–(21).

4. Forced vibration of a cracked CHS beam

Vibrations can be excited by applying a harmonic force along any co-ordinate direction. For an uncracked beam, lateral force will only excite the corresponding lateral displacement (bending modes) and axial force only axial displacement (axial modes). In the case of a cracked beam the vibration modes are coupled. This coupling behaviour can be observed for example by examining the FRFs of the system.

Assuming a transverse harmonic excitation force $F(L, t) = f_0 \cos \omega t$ is applied at the free end of the beam the boundary condition of Eq. (22c) becomes:

$$EIv_1'''(0) = f_0. \tag{30}$$

All other boundary conditions remain identical. The coefficients $A_1, A_2, \ldots, A_{12}$ can now be computed by solving the linear system equation:

$$[Q]\{A\} = \{F\}, \tag{31}$$

where $[Q]$ is the coefficient matrix; $\{F\} = \{0, 0, \ldots f_0, \ldots 0\}^{\mathrm{T}}$. Substituting the solution of $\{A\}$ back into Eqs. (18)–(21) we can get the FRFs $U/F = u(x, \omega)/f_0$, $V/F = v(x, \omega)/f_0$ for longitudinal and lateral vibration, respectively. Fig. 2 shows a typical driving point FRF for the free end of a beam.

5. Analytical simulations

The following parameters are used: beam length 1.5 m, outside diameter 48.3 mm, wall thickness 3.2 mm, Young's modulus 200 GPa and mass density 7850 kg/m^3. The crack location is

assumed to be 0.45 m (30% of total length) from one end. The calculated driving point FRFs of a free end of the beam are shown in Fig. 2. Plot (a) is the lateral FRF for an uncracked beam. Plots (b) and (c) show the lateral FRFs when the crack severity is 10% and 20%, respectively.

As expected the presence of the crack introduces extra peaks into the FRFs. Comparing plots (b) and (c) against (a), one observes that the presence of the crack influences the FRFs in two ways: (i) all natural frequencies are reduced because of loss of stiffness at the crack location; and (ii) an extra peak is introduced as noted on the plots. The natural frequency corresponding to the new peak is close to the uncracked axial natural frequency. This indicates the coupling of lateral and axial vibration. The correlation between the new mode and the axial mode can also be identified by using the modal assurance criterion (MAC) methodology. This is a common modal analysis tool typically used to compare mode shapes [17]. The mode shape correlation is generally displayed as the so-called MAC matrix, where each cell represents the degree of fit between two mode shapes with values between 0 and 1. A value of 1 corresponds to a perfect correlation. In the paper, the MAC matrix is presented by colour-coded patch plot. The size of the individual square also indicates the relative value.

Fig. 3 shows the MAC matrix between the lateral modes of an uncracked and a 10% cracked beam. The first five modes are highly correlated as indicated by high MAC values. However, the sixth mode of the cracked beam does not correlate with any lateral mode of the uncracked beam. On the other hand, the seventh mode of cracked beam is highly correlated to the sixth mode of uncracked beam. This suggests that the sixth mode for the cracked beam is a new mode that corresponds to none of the lateral modes of the undamaged beam. In fact, a comparison with the axial mode of the undamaged beam results in a MAC value of 0.7. The correlation does not indicate a perfect match, since the new mode includes some bending component. This is also the reason for the small frequency shift between the axial mode of the uncracked beam and the new coupled mode.

6. Experimental results

In order to determine the practical feasibility of this approach, it has to be demonstrated that the mode coupling is clearly observable in experimental FRF. Modal tests were conducted for a CHS beam with the dimensions listed above. The beam was suspended by a pair of soft elastic straps simulating free–free boundary conditions. The artificial crack was created by a 0.5 mm thickness hacksaw. The beam was excited using an impulse hammer. This provided excitation covering a frequency range up to 2500 Hz. The responses were measured at one free end while the excitation points were evenly located along the beam. The data acquisition and FFT analysis were implemented by the OR24 analyzer. This is an integrated 4-ch modal testing and analysis tool featuring multiple trigger model, FRF displaying and flexible data storage format. The FRFs were calculated from input and output data using standard H1 estimation [17]. A laptop computer was used as an interface for data acquisition system and for further manipulation of the data.

Both undamaged and damaged CHS beams were tested and the related FRFs and modal shapes were generated. Fig. 4 shows the driving point FRFs for one free end of the uncracked and cracked beam (crack severity is 20% and 40%, respectively). The extra new peak is clearly

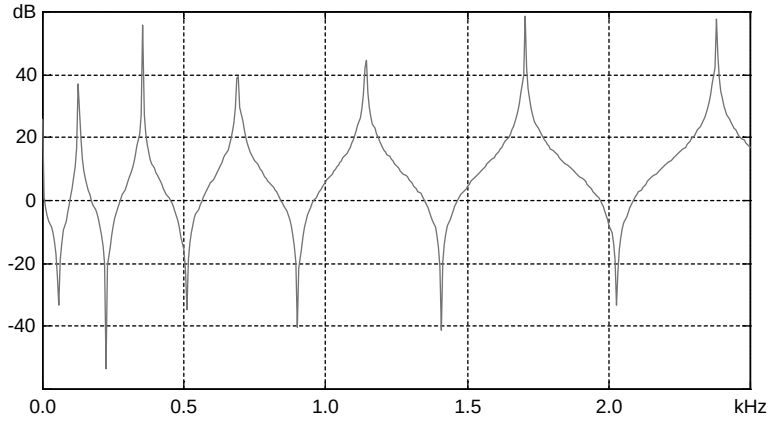

(a) FRF of uncracked CHS beam

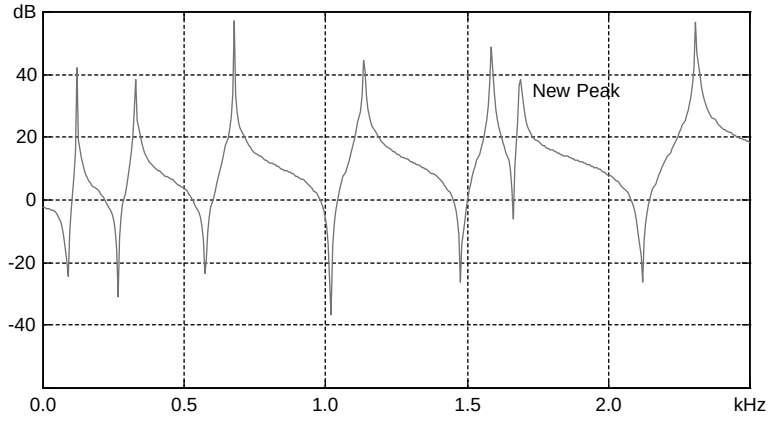

(b) FRF of cracked (10%) CHS beam

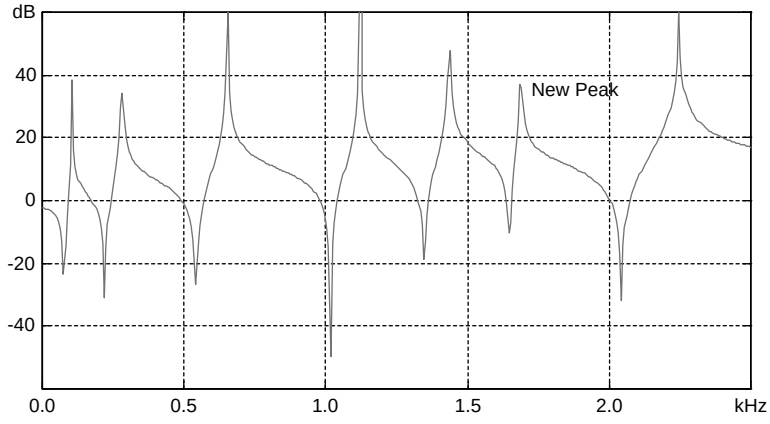

(c) FRF of cracked (20%) CHS beam

Fig. 2. Analytical FRFs of uncracked and cracked CHS beam.

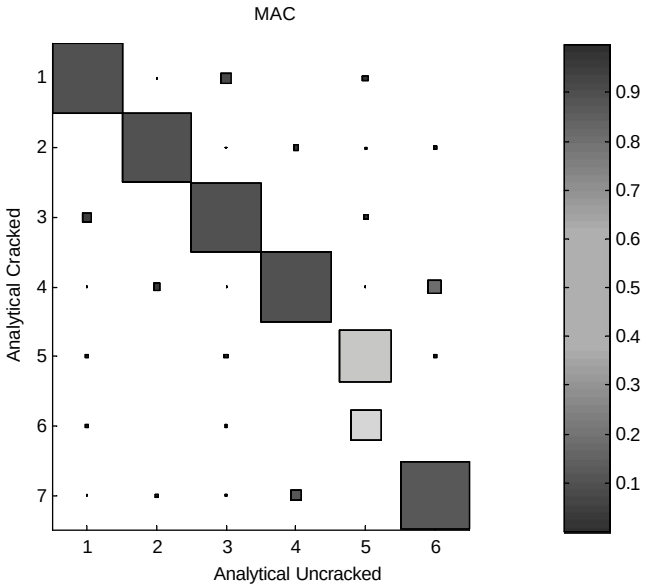

Fig. 3. MAC matrix of uncracked and cracked beam (analytical).

observable at a crack severity of 20%. Obviously, as the crack length is increased the new peak becomes more pronounced. Fig. 5 shows the results of the MAC mode correlation analysis.

The similarity between the experimental results in Fig. 4 and the analytical results displayed in Fig. 2 support the thesis that a coupled response analysis is a valid approach to crack detection in beams. One first should note the good agreement between the measured (Fig. 4a) and the predicted (Fig. 2a) frequencies for the uncracked beam. The amount of shift caused by the introduction of the crack is also similar between the two figures (e.g., cf. Fig. 2c against Fig. 4b).

7. Summary and conclusions

In this paper, we demonstrated the feasibility of a damage detection method that works by detecting the emergence of a new coupled mode in FRFs produced by unidirectional excitation. We used a CHS member as an example to analytically study the free and forced vibration of a cracked CHS beam and then experimentally observe the coupling behaviour of the same structure. Both methods showed that the coupling property was a good indicator of the existence of cracks. The results under different crack severities were compared. The analytical model is more sensitive. A 10% crack causes a new peak at a severity comparable to the other modes in the analytical chart of Fig. 2c. A crack of the same severity, on the other hand, is barely visible on the experimentally obtained chart of Fig. 4b.

The reason for the coupling is the non-diagonal terms introduced into the local flexibility matrix by the presence of a crack. One can observe the coupled response measurements through

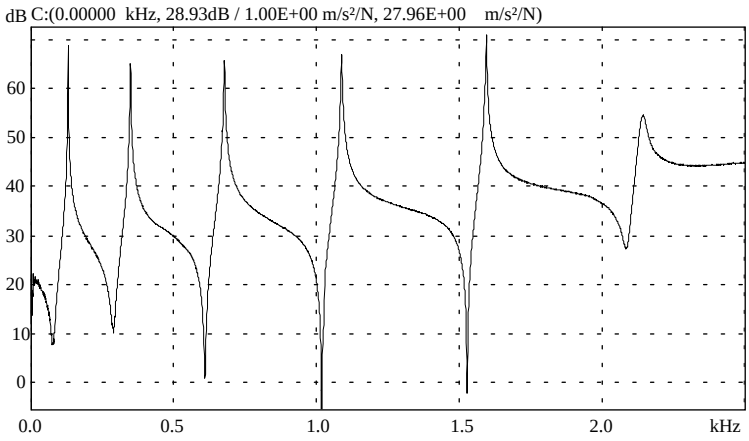

(a) FRF of uncracked CHS beam

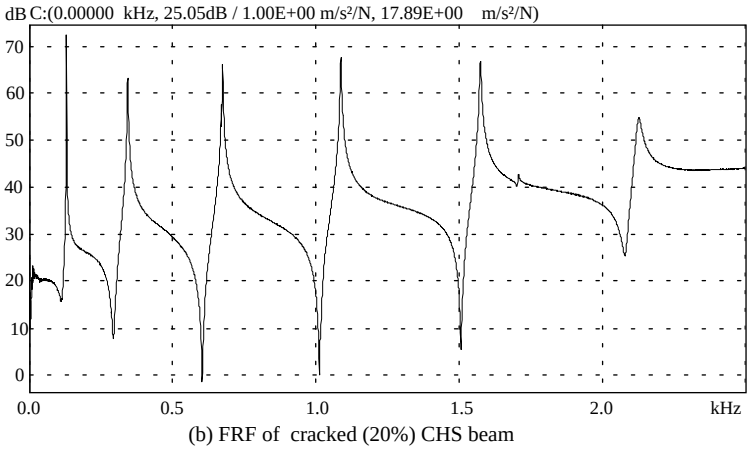

(b) FRF of cracked (20%) CHS beam

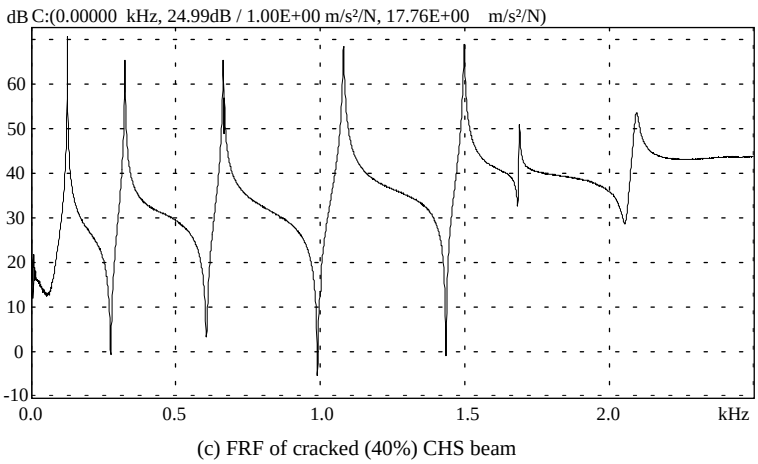

(c) FRF of cracked (40%) CHS beam

Fig. 4. Experimental FRFs of uncracked and cracked CHS beam.

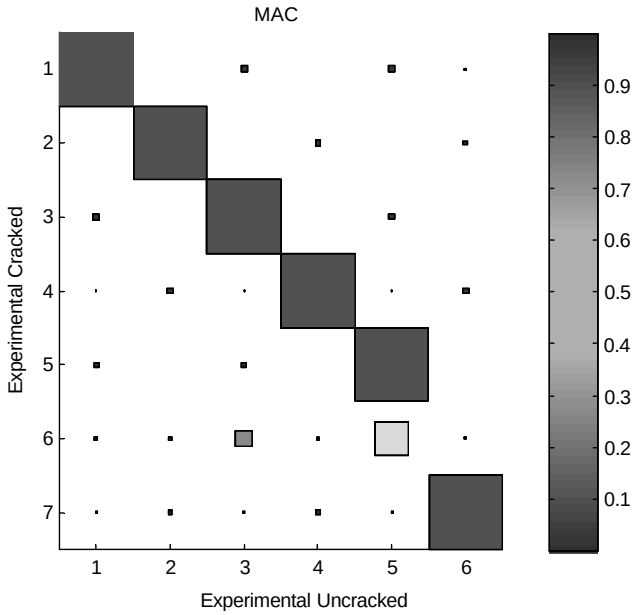

Fig. 5. MAC matrix of uncracked and cracked beam (experimental).

the extra peak in the driving point FRF. The extra peaks on FRF plots suggest the existence of cracks. Before making any decision these extra modes need to be physically interpreted. Standard validation tools such as MAC can be used for this purpose.

Although the results presented here were obtained for free–free beams, the principle equally applies to other beam configurations. A more critical assumption is that of linear fracture mechanics and an open crack model. Further studies are currently performed to explore the application of this approach to more complex structures and fatigue crack identification.

Acknowledgements

The authors would like to thank the CRC for Mining Technology and Equipment (CMTE) and the Department of Mechanical Engineering of the University of Queensland for their support of this project.

Appendix A. Nomenclature

E	Young's modulus
I	moment of inertia
A	cross-sectional area
ρ	mass density
v	the Poisson ratio

$U_i(x,t)$	axial displacement
l	crack location
U_T	strain energy
$J(a)$	strain energy density function
C	local flexibility matrix
K_{mn}	stress intensity factor
Q	characteristic matrix
$V_i(x,t)$	lateral displacement
L	length of the beam

References

[1] A.D. Dimarogonas, Vibration of cracked structures: a state of the art review, Engineering Fracture Mechanics 55 (5) (1996) 831–857.
[2] J. Wauer, On the dynamics of cracked rotors: a literature survey, Applied Mechanics Review 43 (1) (1990) 13–17.
[3] S.W. Doebling, et al., Damage identification and health monitoring of structural and mechanical systems from changes in their vibration characteristics: a literature review, Los Alamos National Laboratory Report, LA-13070-MS, 1996.
[4] T.G. Chondros, A.D. Dimarogonas, Identification of cracks in welded joints of complex structures, Journal of Sound and Vibration 69 (4) (1980) 531–538.
[5] P. Gudmundson, Eigenfrequecy changes of structures due to cracks, notches or other geometrical changes, Journal of Mechanics and Physics of Solids 30 (5) (1982) 339–353.
[6] P. Gudmundson, The dynamic behaviour of slender structures with cross-sectional cracks, Journal of Mechanics and Physics of Solids 31 (4) (1983) 329–345.
[7] P.F. Rizos, N. Aspragathos, Identification of crack location and magnitude in a cantilever beam from the vibration modes, Journal of Sound and Vibration 138 (3) (1990) 381–388.
[8] C.H.J. Fox, The location of defects in structures: a comparison of the use of natrual frequency and mode shape data, Proceedings of the 10th International Modal Analysis Conference, 1992, pp. 522–528.
[9] R.G. Flesch, K. Kernichler, Bridge inspection by dynamic tests and calculations dynamic investigations of lavent bridge, Workshop On Structural Safety Evaluation, 1988, pp. 433–459.
[10] T.L. Anderson, Fracture Mechanics, Fundamentals and Applications, CRC Press, Boca Raton, FL, 1994.
[11] A.D. Dimarogonas, Analytical Methods in Rotor Dynamics, Applied Science Publishers, Essex, 1983.
[12] K.Y. Lam, G.R. Liu, Y.Y. Wang, Time-harmonic response of a vertical crack in plates, Theoretical and Applied Fracture Mechanics 27 (1) (1997) 21–28.
[13] Y.Y. Wang, K.Y. Lam, G.R. Liu, Wave scattering of interior vertical crack in plates and the detection of the crack, Engineering Fracture Mechanics 59 (1) (1998) 1–16.
[14] G.R. Irwin, Fracture Mechanics, Pergamon Press, Oxford, 1960.
[15] J.R. Rice, N. Levy, The part-through surface crack in an elastic plate, Journal of Applied Mechanics 39 (1972) 185–194.
[16] C.A. Papadopoulos, A.D. Dimarogonas, Coupling of bending and tortional vibration of a cracked Timoshenko shaft, Ingenieu-Archiv 57 (1987) 257–266.
[17] D.J. Ewins, Modal Testing: Theory and Practice, Research Study Press, Letchworth, 1984.